

# Multi-Slice Clustering for 3-order Tensor Data

Dina Faneva Andriantsiory, Joseph Ben Geloun, Mustapha Lebbah

Laboratoire d'Informatique de Paris Nord (LIPN)  
Université Sorbonne Paris Nord

**Abstract.** Several methods of triclustering of three dimensional data require the specification of the cluster size in each dimension. This introduces a certain degree of arbitrariness. To address this issue, we propose a new method, namely the multi-slice clustering (MSC) for a 3-order tensor data set. We analyse, in each dimension or tensor mode, the spectral decomposition of each tensor slice, i.e. a matrix. Thus, we define a similarity measure between matrix slices up to a threshold (precision) parameter, and from that, identify a cluster. The intersection of all partial clusters provides the desired triclustering. The effectiveness of our algorithm is shown on both synthetic and real-world data sets.

## 1 Introduction

Consider  $m_1$  individuals with  $m_2$  features and collect the data for each individual-feature pair at  $m_3$  different times. This is an example of a collection of data set with 3 dimensions. Multidimensional data of this kind arise in sundry contexts such as neuroscience [24], genomics data [2,21], computer vision [18] and several other domains [8]. A convenient way to encode such data is given by a 3-order tensor. Because of their augmenting complexity, the mining of higher dimensional data naturally proceeds with the identification of subspaces with specific features. Clustering is one of the most popular unsupervised machine learning methods for extracting relevant information such as structure similarity in data. Thus, several computational methods for clustering multidimensional data, from matrices to higher order tensors, were introduced, see for example the review [8]. For a detailed account of various available methods closer to our present work, see [7,12,6,1,5,3].

A great deal of clustering techniques applied to tensors are based on the formalism of Kolda and Bader [12]. Following that trend, Feizi et al. in [6] proposed four algorithms to select the highly correlated trajectories over one dimension (figure 1b). An extension of that work to select multiple clusters of trajectories is proposed by Andriantsiory et al. in [1]. Later, Wang and collaborators [22] set up partitions in each mode of the tensor and considered the intersection of three clusters from different modes as a block represented by a mean (Multiway clustering). Another method is the so-called CP+k-means, see for instance Papalexakis et al. [15], and Sun and Li [17]. One starts with a CP-decomposition of the tensor into  $R$  rank-1 tensors, and then apply the k-means clustering [23] to the rows of each matrix factor. Similarly, the Tucker+k-means [16] uses a Tucker

decomposition [19] of the tensor and then apply a usual k-means clustering. We will be interested in the improvements of these algorithms in the present work. (Note that the Multiway clustering of Wang et al [22] will approximately behave like the Tucker+k-means in our setting.)

In the usual sense, the triclustering tensor problem aims at computing a triple of subsets of features, individuals and times where the entries of the tensor are strongly similar and have a structure of block (a sub-cube) with higher means (figure 1d). It is considered as a natural generalization and next step of the tensor biclustering method.

In general, the clustering algorithms depend on the number of clusters or the cluster size as data input. Nevertheless, for real data, these inputs might be very difficult to assess from the outset. Another important open issue about the inputs (cluster sizes) concerns the comparison of different clustering results from different parameter inputs. This leads to difficulties in the actual choice of their value. We must mention that the usual clustering algorithms only guarantee a clear distinction between a given cluster and the rest of the data, without guaranteeing the strong correlation within a cluster. One might ask both properties: separation and strong correlation within the cluster.

In this paper, we first bring an answer to the issue of the parameter sizes. Our method concentrates on one dimension of the tensor and studies each matrix slice of that mode. We select the top-eigenvectors of all slices and study a covariance-type matrix associated with those. This guides us towards the selection of an index subset with highly similar features. The input sizes of the cluster are not needed as input of the algorithm. Instead, we set a threshold parameter which gauges the similarity within the cluster. Our method leads to a well-defined triclustering with performance comparable to that of Tensor Folding Spectral (TFS) method [6] and of the Tucker+k-means (for  $k = 2$ ). Finally, we show experimentally, using a similarity index measure within the cluster, that all vectors selected are always strongly correlated, a feature not necessarily shared by the other algorithms.

The paper is organized as follows: in section 2, we address the problem formulation. The description of our method and algorithm is set in section 3. Then, in section 4, we apply our algorithm on synthetic data to compare the coherence of the theory and compare its performance with those of three known clustering algorithms. We also apply the algorithm on a real dataset and extract a tri-cluster. Section 5 summarizes our results. The paper has a companion supplementary material that gathers the proofs of our main theorems that is put at the end of this manuscript.

## 2 Problem formulation

**Notation** – We use  $\mathcal{T}$  to represent the 3-order tensor data and use Matlab notation in next manipulations. For the matrices, we use capital letters:  $M, C, \dots$ , and  $\|M\|$  is the operator norm of  $M$ . The lowercase boldface letters  $\mathbf{x}, \mathbf{v}, \dots$  represent vectors and  $\|\mathbf{x}\|_2$  is the euclidean norm of the vector  $\mathbf{x}$ . For any set

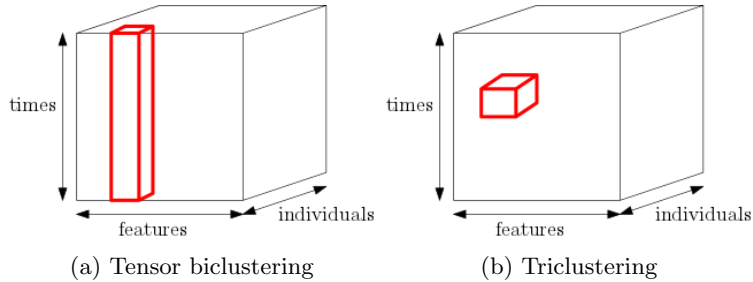


Fig. 1: (a) The tensor biclustering model and (b) The tensor triclustering model.

$J$ ,  $|J|$  denotes the cardinality of  $J$  and  $\bar{J}$  denotes the complementary of  $J$  in a larger set. For an integer  $n > 0$ , we denote  $[n] = \{1, \dots, n\}$ . The asymptotic notation  $a(n) = \mathcal{O}(b(n))$  (res.  $a(n) = \Omega(b(n))$ ) means that, there exists a universal constant  $c$  such that for sufficiently large  $n$ , we have  $|a(n)| \leq cb(n)$  (resp.  $|a(n)| \geq cb(n)$ ).

Let  $\mathcal{T} = \mathcal{X} + \mathcal{Z}$  with  $\mathcal{T} \in \mathbb{R}^{m_1 \times m_2 \times m_3}$ , where  $\mathcal{X}$  is the signal tensor and  $\mathcal{Z}$  is the noise tensor. Consider

$$\mathcal{T} = \mathcal{X} + \mathcal{Z} = \sum_{i=1}^r \gamma_i \mathbf{w}^{(i)} \otimes \mathbf{u}^{(i)} \otimes \mathbf{v}^{(i)} + \mathcal{Z} \quad (1)$$

where  $\forall i, \gamma_i > 0$  stands for the signal strength,  $\mathbf{w}^{(i)} \in \mathbb{R}^{m_1}$ ,  $\mathbf{u}^{(i)} \in \mathbb{R}^{m_2}$  and  $\mathbf{v}^{(i)} \in \mathbb{R}^{m_3}$  are normed vectors, and  $r$  is a number of rank-1 tensor (vector) decomposition of the signal tensor. In this work, we restrict to the case  $r = 1$ .

**Definition 21 (Triclustering)** *The problem of tensor triclustering aims at computing a triple  $(J_1, J_2, J_3)$  of index sets with  $J_i \subset [m_i], i = 1, 2, 3$ , where the entries of  $\mathcal{T}$  are highly correlated (similar).*

To simplify notation, we drop the superscripts  $(i)$  from  $\mathbf{v}^{(i)}$  and from the other vectors. For every  $(j_1, j_2, j_3) \in J_1 \times J_2 \times J_3$ ,  $|\mathbf{w}(j_1)| \leq \delta$ ,  $|\mathbf{u}(j_2)| \leq \delta$  and  $|\mathbf{v}(j_3)| \leq \delta$  for a constant  $\delta > 0$  and  $\mathcal{X}_{j_1, j_2, j_3} = 0$  for each  $(j_1, j_2, j_3)$  outside  $J_1 \times J_2 \times J_3$ . Concerning the noise mode, for  $(j_1, j_2, j_3) \in \bar{J}_1 \times \bar{J}_2 \times \bar{J}_3$ , we assume that the entries of  $\mathcal{Z}$  are i.i.d and have a standard normal distribution. This is the conventional noise model in unsupervised learning method for tensor data [6,4].

### 3 Method

**Multi-slice clustering** – Consider the triclustering problem (1). Using the notation of Kolda and Bader [12], let

$$T_i = \mathcal{T}(i, :, :) = X_i + Z_i, \quad i \in [m_1] \quad (2)$$

be the horizontal (the first mode) matrix slice of the tensor  $\mathcal{T}$ , with  $X_i = \mathcal{X}(i, :, :)$  and  $Z_i = \mathcal{Z}(i, :, :)$ . Similarly, we can define the lateral (the second mode) and the

frontal (the third mode) matrix slices. A way to learn the embedded triclustering is to find the similarity of the slices in each mode. This yields an index subset  $J_i$  for each mode. Now, the collection of  $J_i$  determines the tricluster.

**Definition 31 (Multi-slice clustering (MSC))** *The problem of multi-slice clustering of a 3-order tensor  $\mathcal{T}$  aims at determining and gathering the indices of the matrix slices that are similar in each dimension of the tensor.*

To illustrate the procedure, we will focus on the horizontal slices without loss of generality.

We perform a spectral analysis of

$$C_i = T_i^t T_i, \quad i \in [m_1]. \quad (3)$$

For each  $i \in [m_1]$ ,  $C_i$  represents the symmetric covariance matrix of the  $i$ -th horizontal slice.

For  $i \in J_1$ , equation (1) shows that

$$C_i = (X_i + Z_i)^t (X_i + Z_i) = X_i^t X_i + X_i^t Z_i + Z_i^t X_i + Z_i^t Z_i \quad (4)$$

Taking into consideration (1) and (2), a tensor calculation shows that the matrix  $X_i^t X_i = \lambda_i \mathbf{v}_i \mathbf{v}_i^t$ , where  $\lambda_i = \gamma_i^2 (\mathbf{w}(i))^2 > 0$  is the top eigenvalue of  $X_i^t X_i$  that corresponds to the top eigenvector  $\mathbf{v}_i$ . We re-express  $C_i = \lambda_i \mathbf{v}_i \mathbf{v}_i^t + W_i$  with  $W_i$  the remainder inferred from the equation (4). There is a perturbation bound that shows the norm difference between the top eigenvectors of  $C_i$  and  $\mathbf{v}_i$ , see supplementary material, section 4.

For  $i \notin J_1$ , the expression  $C_i$  (3) becomes the covariance of the noise slice:  $C_i = Z_i^t Z_i$  where each row of  $Z_i$  is real and independently drawn from  $\mathcal{N}_{m_3}(0, I)$ , the  $m_3$ -variate normal distribution with zero mean and the covariance matrix is the identity matrix  $I$ . The matrix  $C_i$  has a white Wishart distribution  $\mathcal{W}_{m_3}(m_2, I)$  [11]. The largest eigenvalue distribution  $\lambda_i$  of  $C_i$  when  $m_2 \rightarrow \infty, m_3 \rightarrow \infty$  and  $\frac{m_2}{m_3} \rightarrow \text{cst} > 1$ , obeys the limit in the distribution sense

$$\frac{\lambda_i - \mu_{m_2 m_3, 1}}{\sigma_{m_2 m_3, 1}} \xrightarrow{\mathcal{D}} F_1 \quad (5)$$

where  $F_1$  is the Tracy-Widom (TW) cumulative distribution function (cdf), and

$$\begin{aligned} \mu_{m_2 m_3, 1} &= (\sqrt{m_2 - 1} + \sqrt{m_3})^2 \\ \sigma_{m_2 m_3, 1} &= \sqrt{\mu_{m_2 m_3, 1}} \left( \frac{1}{\sqrt{m_2 - 1}} + \frac{1}{\sqrt{m_3}} \right)^{\frac{1}{3}} \end{aligned} \quad (6)$$

As stated in [11], the expression (5) applies equally well if  $m_2 < m_3$  when  $m_2 \rightarrow \infty, m_3 \rightarrow \infty$  and if the role of  $m_2$  and  $m_3$  are reversed in the expression of  $\mu_{m_2 m_3, 1}$  and  $\sigma_{m_2 m_3, 1}$ . Although (5) is true in the limit, it is also shown that it provides a satisfactory approximation from  $m_2, m_3 \geq 10$ . Our following computations lie above that approximation. In the next developments, we drop the subscript  $(m_2 m_3, 1)$  in  $\mu_{m_2 m_3, 1}$  and  $\sigma_{m_2 m_3, 1}$ , so we will only use  $\mu$  and  $\sigma$ .

The covariance matrix  $C_i$  defines both the spread (variance) and the orientation (covariance) of our slice data. We are interested in the vector that represents the covariance matrix and its magnitude. The idea is to find the vector that points into the direction of the largest spread of the data  $(\lambda_i, \mathbf{v}_i)$ .

We now detail our strategy. Since the signal tensor has rank one, we undertake the analysis of the relation between two slices. We seek for criteria characterizing high similarity between the top eigenvectors and top eigenvalues of all slices. A first necessary condition for achieving a MSC is to target high correlation between the top eigenvectors of the slices. To proceed, we build the covariance matrix  $C = (c_{ij})$  of the top eigenvectors with signs removed. We claim that two slices  $i$  and  $j$  are similar if the corresponding coefficient  $c_{ij}$  is large enough. At this stage, we set up our precision parameter  $\epsilon$  that determines the correlation strength between slices and, at a threshold, call these slices  $\epsilon$ -similar. We introduce a vector  $\mathbf{d}$  the coordinate  $d_i$  of which is the marginal sum of  $C$  associated with the slice  $C_i$ . Any slice  $i$  that belongs to the cluster can be regarded as a centroid. Any other slice  $j$  in the same cluster is highly similar to  $i$  and therefore will contribute to  $d_i$ . An increasing number of such  $j$  makes  $d_i$  larger. So, for  $i$  in the cluster and  $j$  outside the cluster, we have  $d_i > d_j$  with high probability. The next step amounts to set up a notion of distance between the cluster and the rest. We consider this as a criterion to determine the initial cluster. Then, we use the parameter  $\epsilon$  to fit the right cluster.

For each slice, the relation (3) holds for  $i = 1, \dots, m_1$ . Let  $\underline{\lambda}_i$  be the top eigenvalue and  $\tilde{\mathbf{v}}_i$  be the top eigenvector of  $C_i$ . We construct the matrix

$$V = [\tilde{\lambda}_1 \tilde{\mathbf{v}}_1 \cdots \tilde{\lambda}_{m_1} \tilde{\mathbf{v}}_{m_1}] \quad (7)$$

where we set  $\tilde{\lambda}_i$  to  $\underline{\lambda}_i/\lambda, \forall i \in [m_1]$ , and  $\lambda = \max(\underline{\lambda}_1, \dots, \underline{\lambda}_{m_1})$ . Let  $C$  be the matrix with each entry  $(c_{ij})_{i,j \in [m_1]}$  defined by

$$c_{ij} = |\langle \tilde{\lambda}_i \tilde{\mathbf{v}}_i, \tilde{\lambda}_j \tilde{\mathbf{v}}_j \rangle| = \tilde{\lambda}_i \tilde{\lambda}_j |\langle \tilde{\mathbf{v}}_i, \tilde{\mathbf{v}}_j \rangle| \leq 1 \quad (8)$$

$C$  is a symmetric matrix and its columns are not unit vectors. Note also that  $C$  is related to the covariance matrix  $V^t V$  in which we take the absolute values of the entries.

**Definition 32 ( $\epsilon$ -similarity)** *The slice  $i$  and  $j$  are called  $\epsilon$ -similar, if for a small  $\epsilon > 0$  we have,*

$$c_{ij} \geq 1 - \epsilon/2 \quad (9)$$

Let  $\mathbf{d} = (d_1, \dots, d_{m_1})$  a real vector defined by the marginal sum in  $C$ :  $\forall i \in [m_1]$

$$d_i = \sum_{j \in [m_1]} c_{ij} \quad (10)$$

Using (9) and (10), the elements of  $J_1$  are indices  $i \in [m_1]$  which define pairwise  $\epsilon$ -similar slices and thus obeys

$$d_i \geq l(1 - \epsilon/2) \quad (11)$$

where  $l = |J_1|$ . Note that in the previous equation  $l$  is unknown (does not define a final criterion to select the indices of the cluster). However, it already shows that  $d_i$  is bounded from below and non negligible as soon as  $l$  is large enough. The algorithm aims at computing  $l$ , in such way that only  $\epsilon$ -similar slices that satisfy (11) define the cluster  $J_1$ . The following statements demonstrate that this event happens with overwhelming probability.

**Theorem 31** *Let  $l = |J_1|$ , assume that  $\sqrt{\epsilon} \leq \frac{1}{m_1 - l}$ .  $\forall i, n \in J_1$ , for  $\lambda = \Omega(\mu)$ , there is a constant  $c_1 > 0$  such that*

$$|d_i - d_n| \leq l \frac{\epsilon}{2} + \sqrt{\log(m_1 - l)} \quad (12)$$

*holds with probability at least  $1 - e(m_1 - l)^{-c_1}$ .*

*Proof.* See supplementary material, section 5.2.

We inspect closer the previous inequality, and use  $\sqrt{\epsilon} \leq 1/(m_1 - l)$  to write  $|d_i - d_n| \leq l \frac{\epsilon}{2} + \sqrt{\frac{1}{2} |\log \epsilon|}$ . Thus, as the logarithm may indeed increase, to choose a smaller  $\epsilon$  might not lead to a smaller radius of the cluster. There is therefore an unknown threshold for  $\epsilon$  that will lead to the best clustering. Another remark is the following: since we must determine  $l$  by iteration and that value turns out to decrease, the relation (38) holds with a higher probability at each step of the iteration.

**Theorem 32** *For  $i \in \bar{J}_1$ , if  $\lambda = \Omega(\mu m_1)$ ,*

$$d_i \leq \frac{l}{m_1} + \sqrt{\log(m_1 - l)} \quad (13)$$

*with probability at least  $1 - e(m_1 - l)^{-c_1}$  with  $c_1 > 0$ .*

*Proof.* See supplementary material, section 5.2.

The distance  $\text{dist}(A, B)$  between two sets of real numbers  $A$  and  $B$  is naturally defined as  $\min\{|x - y| : x \in A, y \in B\}$ . We introduce  $d(J_1) = \{d_i : i \in J_1\}$ , and  $d(\bar{J}_1) = \{d_i : i \in \bar{J}_1\}$ .

**Corollary 1** *Let  $J_1 \subset [m_1]$  the set of all indices of the cluster in the first dimension. Then*

$$\text{dist}(d(J_1), d(\bar{J}_1)) \geq l \left(1 - \frac{\epsilon}{2} - \frac{1}{m_1}\right) - \sqrt{\log(m_1 - l)}, \quad (14)$$

*with probability at least  $1 - e(m_1 - l)^{-c_1}$ , with  $c_1 > 0$ .*

*Proof.* This is an easy calculation starting from (11) and using theorem 2.

---

**Algorithm 1** Multi-slice clustering for 3-order tensor
 

---

**Input:** 3-order tensor  $\mathcal{T} \in \mathbb{R}^{m_1 \times m_2 \times m_3}$ , real parameter  $\epsilon > 0$

**Output:** sets  $J_1, J_2$  and  $J_3$

- 1: **for**  $j$  in  $\{1, 2, 3\}$  **do**
- 2:   Initialize the matrix  $M$
- 3:   Initialize  $\lambda_0 \leftarrow 0$
- 4:   **for**  $i$  in  $\{1, 2, \dots, m_j\}$  **do**
- 5:     Compute :  $C_i \leftarrow T_i^t T_i$
- 6:     Compute the top eigenvalue and eigenvector  $(\lambda_i, \mathbf{v}_i)$  of  $C_i$
- 7:     Compute  $M(:, i) \leftarrow \lambda_i * \mathbf{v}_i$
- 8:     **if**  $\lambda_i > \lambda_0$  **then**
- 9:        $\lambda_0 \leftarrow \lambda_i$
- 10:    **end if**
- 11:   **end for**
- 12:   Compute :  $V \leftarrow M / \lambda_0$
- 13:   Compute :  $C \leftarrow |V^t V|$
- 14:   Compute :  $\mathbf{d}$  the vector marginal sum of  $C$  and sort it
- 15:   Initialization of  $J_j$  using the maximum gap in  $\mathbf{d}$  sorted
- 16:   Compute :  $l \leftarrow |J_j|$
- 17:   **while** not convergence of the elements of  $J_j$  (theorem 1) **do**
- 18:     Update the element of  $J_j$  (excluding  $i$  s.t.  $d_i$  is the smallest value that violates theorem 1)
- 19:     Compute  $l$
- 20:   **end while**
- 21: **end for**

---

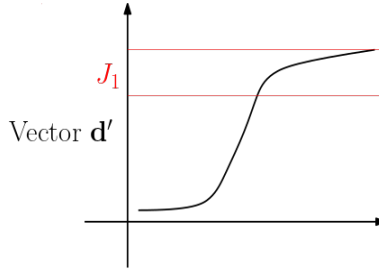


Fig. 2: Representation of the vector  $\mathbf{d}$  after reordering its elements in ascending order.

The corollary 1 proves that the distance  $\text{dist}(d(J_1), d(\bar{J}_1))$  increases when the number of elements that belong to the cluster increases.

Consider,  $\forall i \in [m_3], d'_i \in \{d_1, \dots, d_{m_3}\}$ , the sequence of  $d_i$  ordered in increasing values,  $d'_1 \leq d'_2 \leq \dots \leq d'_{m_3}$  and  $\mathbf{d}' = (d'_1, \dots, d'_{m_3})$ . The figure 2 represents the global view of the vector  $\mathbf{d}'$  structure.  $J_1$  defines the highest indices of the vector  $\mathbf{d}'$ . Figure 2 exhibits the fact corollary 1 selects the indices of  $J_1$  from the remaining indices with lower value. Our algorithm uses the differences between two consecutive values of  $d'_i$  to detect the gap whose corollary 1 ensures the existence with high probability.

**Computational complexity** – A few words on the complexity of our algorithm is in order. To simplify the evaluation, we require  $m_i \in \Theta(n)$  for  $i = 1, 2, 3$ . The algorithm 1 has a complexity class  $\mathcal{O}(n^3)$  that is comparable with the complexity of other triclustering algorithms. One may be puzzled about the cost of the last repeat loop depending on a convergence parameter. However, there is no issue with that since  $l$  decreases at each turn. The convergence condition evaluates at most as  $\mathcal{O}(l^2)$ , and so this loop costs at most  $\mathcal{O}(l^3) \subset \mathcal{O}(n^3)$ .

## 4 Experiments

To evaluate the quality of the clustering yield by the algorithm, we first use two indices suitable for synthetic data, namely, the recovery rate, see [6], and the Adjusted Random Index (ARI) in [9]. Then, we also discuss the quality of the cluster with respect to the data similarity.

### 4.1 Synthetical results

Here, we evaluate the performance of the MSC algorithm on synthetic datasets. To generate the input tensor  $\mathcal{T}$ , we fix the three sets  $J_1, J_2$ , and  $J_3$ , and the entries of the vectors  $\mathbf{v}, \mathbf{u}$  and  $\mathbf{w}$  in (1) equal to  $1/\sqrt{|J_1|}, 1/\sqrt{|J_2|}$  and  $1/\sqrt{|J_3|}$ , respectively, in the cluster and zero outside the cluster. The noise is chosen standard normal distributed. The quality of the cluster result is evaluated by the recovery rate in each dimension and then we perform a mean of these index

measures. Furthermore, we use a similarity index (sim) that measures the quality of the correlation between the vectors of the cluster:

$$\text{sim} = \frac{1}{3} \sum_{r=1}^3 \frac{1}{J_r^2} \sum_{i,j \in J_r} c_{ij} \leq 1 \quad (15)$$

Thus, the similarity index will help us to assess the quality of the clustering procedure.

In our simulations, we consider  $m_1 = m_2 = m_3 = 50$  and  $|J_1| = |J_2| = |J_3| = 10$ . Hence, with a fixed value of  $\epsilon$ , we variate the value of  $\gamma$  to see the coherence of theorem 1 with the experiment. In the synthetic data,  $\frac{1}{(m_1-l)^2} \approx 0.00062$ . However, if the chosen  $\epsilon$  does not verify the hypothesis of theorem 1, the last selected cluster is returned. For given values of  $\gamma$  (1), we perform 10 times the computation (re-sampling only the noise) then we compute the mean of the cluster quality (recovery rate) and the similarity (sim) of the output for the three modes. The results are shown in figure 3 with the standard deviations (std) of each measure at each  $\gamma$ .

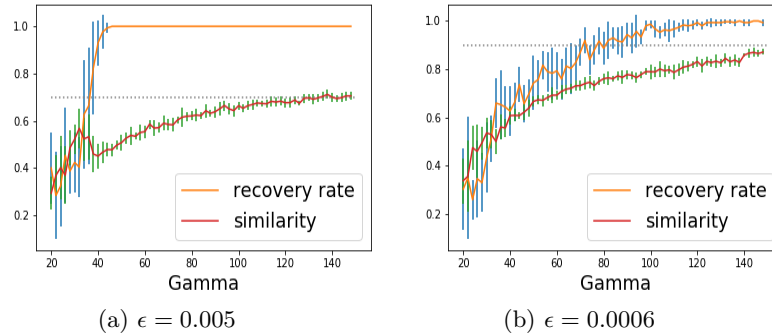


Fig. 3: Recovery rate of the MSC method with  $\gamma \in [20, 150]$ : (a) with  $\epsilon = 0.005$  and (b) with  $\epsilon = 0.0006$ .

For a range of values of  $\gamma$ , the recovery rate of figure 3 (a) increases faster than that of the figure (b). For the larger value of  $\epsilon$  preventing to enter in the while loop, the algorithm reaches a high recovery rate (almost 1) very fast (with  $\gamma = 50$ ) but note that the similarity within the cluster is low (sim= 0.5). However, for the same value of  $\gamma = 50$ , with a smaller  $\epsilon$  that obeys the hypothesis of theorem 1, some indices are removed in the cluster, see figure 3 (b), to guarantee the similarity between the selected indices. As a result, we have a smaller recovery rate equals to 0.7 and sim= 0.65. Increasing the signal, the recovery rate and the similarity are remarkably increased to reach high values. Thus, we have successfully tied the recovery rate with the similarity index.

## 4.2 Comparison with existing methods

In this section, we perform two comparisons. On one hand, we compare the MSC and CP+k-means and Tucker+k-means' methods. We use the same construction and data as in the previous experiment. Referring to [13], the CP and Tucker decompositions deliver factor matrices for each mode and then we apply the k-means' method to the resulting factor matrices. In our case, we use k-means with  $k = 2$ . The ARI serves as a comparison tool of the quality of the results obtained by the different algorithms. We additionally compute the mean squared error (MSE) of the sub-cube cluster as a similarity test of the cluster data. On the other hand, we use the MSC to find a tensor biclustering and compare its performance with the TFS method. To do so, the MSC needs some light adjustments: the clustering is done on 2 modes and is not performed on the third mode that will define the trajectory indices. We generate the same dataset of [6] (section 4.1 therein) with  $m_3 = 50, m_1 = m_2 = 70$  and  $|J_1| = |J_2| = 10$  where  $J_1$  and  $J_2$  represent the two sets of indices in the first and second modes, respectively, that represent the correlated trajectories. We use the recovery rate and the correlation mean of trajectories to evaluate the inference quality of the results in both methods.

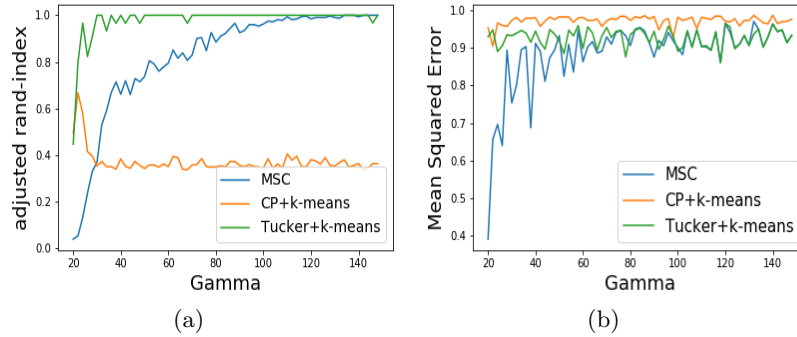


Fig. 4: (a) ARI of MSC ( $\epsilon = 0.0006$ ), CP+k-means and the Tucker+k-means ( $k = 2$ ). (b) MSE of the sub-cube cluster.

In figure 4a, we observe that the Tucker+k-means is the fastest method to find the best cluster but note that the ARI is not stable for  $\gamma < 50$  (a lot of fluctuations that we omit in the figure). The MSC reaches an  $\text{ARI} \geq 0.7$  for  $\gamma = 50$  and becomes close to 0.9 for  $\gamma \geq 75$  and proves to be much stable. As we expected, the ARI of the MSC grows a bit slower than the Tucker+k-means because it is devised to select only the most similar slices in each mode. But at reasonable signal strength, it becomes comparable with the Tucker+k-means. In any case, the CP+k-means is outperformed because it remains stationary even if the value of  $\gamma$  increases. Figure 4b shows the MSE of the different methods.

As expected, the MSC has the best MSE for  $\gamma < 75$ , whereas it fits with that of the Tucker+k-means for  $\gamma \geq 80$ . We can conclude that the MSC is certainly a significant clustering algorithm.

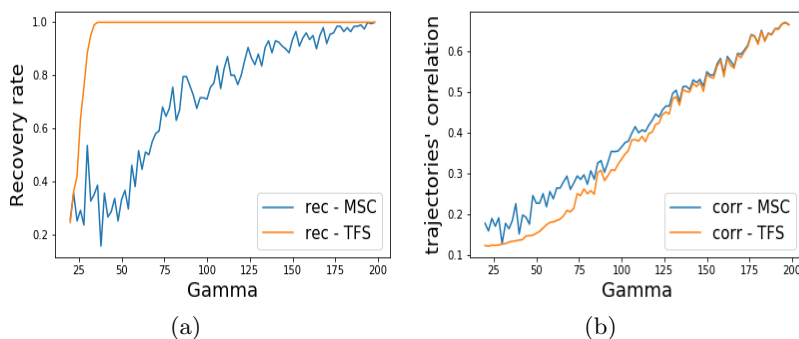


Fig. 5: Recovery rates (rec) and correlation mean (corr) for MSC and TFS.

In the figure 5, we observe that the TFS reaches the highest recovery rate faster than the MSC method with  $\epsilon = 0.00027$  (but remember that the TFS method takes the cardinality  $|J_1| \times |J_2|$  as an input parameter). The recovery rate of the MSC grows slowly but reaches a remarkable good rate at  $\gamma = 125$ . We recall that the TFS method aims at selecting highly correlated trajectories. Nevertheless, as shown in figure 5, for  $\gamma < 120$ , the trajectories which are selected have a very weak correlation mean and thus are not highly correlated. In contrast, as we planned, the correlation mean and recovery rate of the MSC increase together. This comparison shows that, combining both performances, the MSC is certainly a more relevant method for clustering similar trajectories in a 3-order tensor compared to the TFS.

### 4.3 Real dataset

We undertake now the study of the flow injection analysis (FIA) dataset [14] with size 12 (samples)  $\times$  100 (wavelengths)  $\times$  89 (times). The MSC algorithm is tested with different values of  $\epsilon \in [0.005, 0.00001]$ . The cardinality of the cluster decreases and stabilizes for  $\epsilon \in [0.00013, 0.00001]$ . Therefore, we choose  $\epsilon = 0.00013$ . Table 1 presents the indices of similar slices in each mode and the maximum of the Frobenius norm of the difference between them ( $\max_{i,j} \|slice(i) - slice(j)\|_F$  for  $i, j$  in the cluster mode).

We will show that this defines a good 3D cluster with highly correlated vectors by adding a new element in each cluster mode and then experimentally demon-

mode	Indices of similar slices	Max Frobenius norm
mode-1	10, 11	3.08616
mode-2	39, 40, 41, 42, 43	0.40307
mode-3	45, 46, 47, 48, 49, 50, 51, 52	1.05795

Table 1: The similar slices in each mode with the maximum Frobenius norm of the difference between two slices within each mode.

strate that the correlation in the cluster decreases while the MSE of the cluster increases.

Table 2 exhibits the similarity between the fibers (trajectories) by letting one mode free and computing the correlation mean of all fibers from the two clusters of the remaining modes. Moreover, we compute also the MSE of the triclustering

mode	Fibers' correlation
mode-1	0.99915
mode-2	0.97164
mode-3	0.99059

Table 2: Fibers' correlation in each mode and the MSE of the triclustering.

(sub-cube) and obtain  $\text{MSE} = 0.48360$ .

Now, we evaluate the quality of cluster presented in table 1 and 2. To do so, for each mode  $i = 1, 2, 3$ , we add one index, randomly selected, to the cluster set  $i$ , and perform the measurements. This is repeated 60 times (this is the experiment E- $i$ ). At each time, we compute the maximum Frobenius norm of the slice differences, the correlation of the fibers and the MSE of the triclustering. At the end, we select the minimum for all calculations of the Frobenius norms and of the MSE, and the mean of the fibers' correlation. The results are reported in table 3.

E-mod	Frobenius norm	Fibers' correlation	MSE of triclustering
E-1	3.17592	0.83039	0.49257
E-2	3.83777	0.86484	0.51133
E-3	4.86486	0.84928	1.19725

Table 3: Results of the experiments E-1, E-2 and E-3.

We observe, comparing with the above tables and previous MSE of 0.48360, that the Frobenius norm and MSE increase and the fibers' correlation decreases. In short, adding a new element in the output cluster decreases its quality. Hence, the MSC has remarkable performance for detecting a 3D cluster, with strongly similar slices and and strongly correlated fibers in this real dataset.

## 5 Conclusion and future work

The majority of the clustering algorithms depends on parameters which correspond to a given number of clusters or a given number of elements assigned to a cluster. Such parameters do not guarantee the most accurate clusters. We have introduced a new clustering method, the MSC, for 3-order tensor dataset that tackles this issue by using a threshold parameter  $\epsilon$  to carry out the cluster selection and refinement. Our main results state in probabilistic terms (theorems 1) that show the algorithm effectiveness. The experimental validation demonstrates that our algorithm performs well. We have comparable performance (ARI) with the Tucker+k-means, and, adapted to biclustering, with TFS. Moreover, our algorithm guarantees strong correlation/similarity in the triclustering, even at small signal strength, a property that is largely not verified for many algorithms in particular TFS and Tucker+k-means. Concerning real data sets, the new algorithm has located a 3D cluster with highly similar slices and fibers. We note that MSC can be used also to detect the outlier slices in the dataset. A possible fruitful avenue of research would be to select a set of most dominant eigenvectors in each slice to define a multi-clustering. Such a multi-clustering could be compared with contemporary approaches such as the multi-way clustering for higher dimensional data. This deserves full-fledged investigation.

## References

1. Andriantsiory, D., Lebbah, M., Azzag, H., Beck, G.: Algorithms for an efficient tensor biclustering. U. L., Lauw H. (eds) Trends and Applications in Knowledge Discovery and Data Mining. PAKDD 2019 **11607** (2019)
2. Ardlie, K., DeLuca, D., Segrè, A., Sullivan, T., Young, T., Gelfand, E., Trowbridge, C., Maller, J., Tukiainen, T., Lek, M., Ward, L., Kheradpour, P., Iriarte, B., Meng, Y., Palmer, C., Esko, T., Winckler, W., Hirschhorn, J., Kellis, M., Lockhart, N.: The genotype-tissue expression (gtex) pilot analysis: Multitissue gene regulation in humans. *Science* **348**, 648–660 (05 2015)
3. Bach, F.R., Jordan, M.I.: Learning spectral clustering. Tech. Rep. UCB/CSD-03-1249, EECS Department, University of California, Berkeley (Jun 2003)
4. Cai, T.T., Liang, T., Rakhlin, A.: Computational and statistical boundaries for submatrix localization in a large noisy matrix. *The Annals of Statistics* **45**(4) (Aug 2017). <https://doi.org/10.1214/16-aos1488>
5. Carson, T., Mixon, D.G., Villar, S.: Manifold optimization for k-means clustering. In: 2017 International Conference on Sampling Theory and Applications (SampTA). pp. 72–77 (2017)

6. Feizi Soheil, Javadi Hamid, T.D.: Tensor biclustering. In: Guyon, I., Luxburg, U.V., Bengio, S., Wallach, H., Fergus, R., Vishwanathan, S., Garnett, R. (eds.) *Advances in Neural Information Processing Systems*. vol. 30, pp. 1311–1320. Curran Associates, Inc. (2017)
7. Friedlander, M.P., Hatz, K.: Computing non-negative tensor factorizations. *Optimization Methods and Software* **23**(4), 631–647 (2008). <https://doi.org/10.1080/10556780801996244>
8. Henriques, R., Madeira, S.C.: Triclustering algorithms for three-dimensional data analysis: A comprehensive survey. *ACM Comput. Surv.* **51**(5) (Sep 2018). <https://doi.org/10.1145/3195833>
9. Hubert L., A.P.: Comparing partitions. *Journal of Classification* **2**, 193–218 (1985). <https://doi.org/10.1007/BF01908075>
10. J.D. Vlok, J.O.: Analytic approximation to the largest eigenvalue distribution of a white wishart matrix. *IET Communications* **6**, 1804–1811(7) (August 2012)
11. Johnstone, I.M.: On the distribution of the largest eigenvalue in principal components analysis. *Annals of Statistics* **29**(2), 295–327 (04 2001). <https://doi.org/10.1214/aos/1009210544>
12. Kolda, T.G., Bader, B.W.: Tensor decompositions and applications. *SIAM Review* **51**, 455–500 (2009)
13. Kolda, T.G., Sun, J.: Scalable tensor decompositions for multi-aspect data mining. In: *ICDM 2008: Proceedings of the 8th IEEE International Conference on Data Mining*. pp. 363–372 (2008). <https://doi.org/10.1109/ICDM.2008.89>
14. Norgaard, C, R.: Rank annihilation factor analysis applied to flow injection analysis with photodiode-array detection (1994), <http://www.models.life.ku.dk/FlowInjection>, chemometrics and Intelligent Laboratory, Systems 23:107
15. Papalexakis, E.E., Sidiropoulos, N.D., Bro, R.: From k-means to higher-way co-clustering: Multilinear decomposition with sparse latent factors. *IEEE Transactions on Signal Processing* **61**(2), 493–506 (2013). <https://doi.org/10.1109/TSP.2012.2225052>
16. Sun, J., Tao, D., Faloutsos, C.: Beyond streams and graphs: Dynamic tensor analysis. In: *Proceedings of the 12th ACM SIGKDD International Conference on Knowledge Discovery and Data Mining*. p. 374–383. KDD '06, Association for Computing Machinery, New York, NY, USA (2006). <https://doi.org/10.1145/1150402.1150445>, <https://doi.org/10.1145/1150402.1150445>
17. Sun, W.W., Li, L.: Dynamic tensor clustering. *Journal of the American Statistical Association* **114**(528), 1894–1907 (2019). <https://doi.org/10.1080/01621459.2018.1527701>, <https://doi.org/10.1080/01621459.2018.1527701>
18. Tang, Y., Salakhutdinov, R., Hinton, G.: Tensor analyzers. In: Dasgupta, S., McAllester, D. (eds.) *Proceedings of the 30th International Conference on Machine Learning*. *Proceedings of Machine Learning Research*, vol. 28, pp. 163–171. PMLR, Atlanta, Georgia, USA (17–19 Jun 2013)
19. Tucker, R., L.: Some mathematical notes on three-mode factor analysis. *Psychometrika* **31**, 279–311 (1966). <https://doi.org/10.1007/BF02289464>
20. Vershynin, R.: Introduction to the non-asymptotic analysis of random matrices. arXiv e-prints arXiv:1011.3027 (Nov 2010)
21. Wang, M., Fischer, J., Song, Y.: Three-way clustering of multi-tissue multi-individual gene expression data using semi-nonnegative tensor decomposition. *The Annals of Applied Statistics* **13**, 1103–1127 (06 2019). <https://doi.org/10.1214/18-AOAS1228>

22. Wang, M., Zeng, Y.: Multiway clustering via tensor block models. In: Wallach, H., Larochelle, H., Beygelzimer, A., d'Alché-Buc, F., Fox, E., Garnett, R. (eds.) *Advances in Neural Information Processing Systems*. vol. 32. Curran Associates, Inc. (2019)
23. Wilkin, G.A., Huang, X.: K-means clustering algorithms: Implementation and comparison. In: *Second International Multi-Symposiums on Computer and Computational Sciences (IMSCCS 2007)*. pp. 133–136 (2007). <https://doi.org/10.1109/IMSCCS.2007.51>
24. Zhou, H., Li, L., Zhu, H.: Tensor regression with applications in neuroimaging data analysis. *Journal of the American Statistical Association* **108**(502), 540–552 (2013). <https://doi.org/10.1080/01621459.2013.776499>, PMID: 24791032

# Multi-Slice Clustering for 3-order Tensor Data - Supplementary Material

Dina Faneva Andriantsiory, Joseph Ben Geloun, Mustapha Lebbah

Laboratoire d'Informatique de Paris Nord (LIPN)  
Université Sorbonne Paris Nord

**Abstract.** This document provides a supplementary material to the manuscript “Multi-Slice Clustering for 3-order Tensor Data”. It gathers the proof of its main statements. In particular, we prove that within a 3-cluster selected by the Multi-Slice Clustering method, the similarity of data holds with high probability.

## 1 Notation

We use  $\mathcal{T}$  to represent the 3-order tensor data, see figure 1a. We also use the Matlab notation in the next manipulations. For matrices, we use capital letters:  $M, C, \dots$ , and  $\|M\|$  is the operator norm of  $M$ . The lowercase boldface  $\mathbf{x}, \mathbf{v}, \dots$  represent vectors and  $\|\mathbf{x}\|_2$  is the euclidean norm of the vector  $\mathbf{x}$ . For any set  $J$ ,  $|J|$  denotes the cardinality of  $J$  and  $\bar{J}$  denotes the complementary of  $J$  in a larger set. For an integer  $n > 0$ , we denote  $[n] = \{1, \dots, n\}$ . The asymptotic notation  $a(n) = \mathcal{O}(b(n))$  (res.  $a(n) = \Omega(b(n))$ ) means that, there exists a universal constant  $c$  such that for sufficiently large  $n$ , we have  $|a(n)| \leq cb(n)$  (resp.  $|a(n)| \geq cb(n)$ ).

## 2 Problem formulation

Let  $\mathcal{T} = \mathcal{X} + \mathcal{Z}$  with  $\mathcal{T} \in \mathbb{R}^{m_1 \times m_2 \times m_3}$ , where  $\mathcal{X}$  is the signal tensor and  $\mathcal{Z}$  is the noise tensor. Consider

$$\mathcal{T} = \mathcal{X} + \mathcal{Z} = \sum_{i=1}^r \gamma_i \mathbf{w}^{(i)} \otimes \mathbf{u}^{(i)} \otimes \mathbf{v}^{(i)} + \mathcal{Z} \quad (1)$$

where  $\forall i, \gamma_i > 0$  stands for the signal strength,  $\mathbf{w}^{(i)} \in \mathbb{R}^{m_1}$ ,  $\mathbf{u}^{(i)} \in \mathbb{R}^{m_2}$  and  $\mathbf{v}^{(i)} \in \mathbb{R}^{m_3}$  and  $r$  is a number of rank-1 tensor (vector) decomposition of the signal tensor. We shall restrict to the case  $r = 1$ .

**Definition 1 (Triclustering).** *The problem of tensor triclustering aims at computing a triple  $(J_1, J_2, J_3)$  of index sets with  $J_1 \subset [m_1]$ ,  $J_2 \subset [m_2]$  and  $J_3 \subset [m_3]$ , where the entries of  $\mathcal{T}$  are similar.*

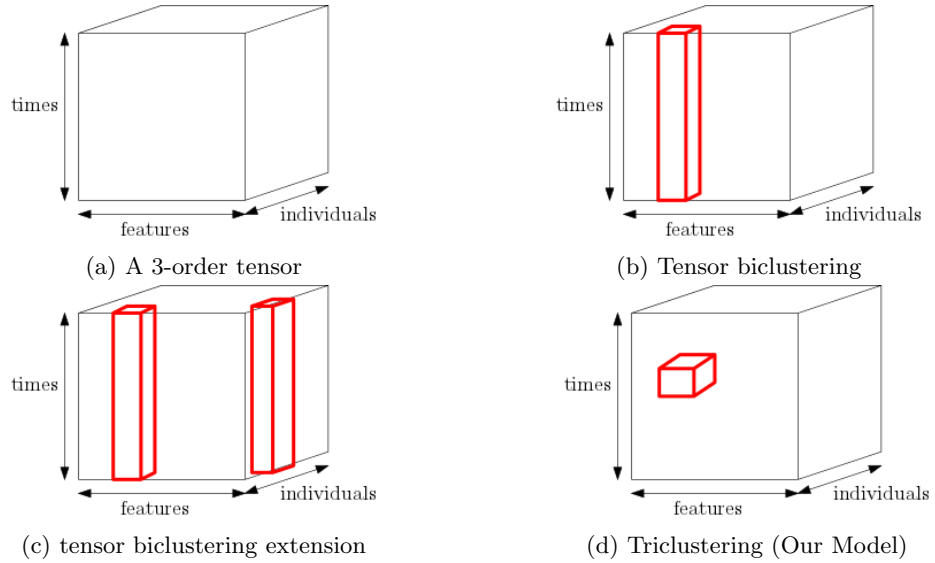


Fig. 1: (a) Representation of a 3-order tensor data set. (b) The tensor biclustering problem. (c) Multiple tensor biclustering [6]. (d) The triclustering problem.

To simplify the notation, we drop the superscripts  $(i)$  from  $\mathbf{v}^{(i)}$  and from the other vectors. For every  $(j_1, j_2, j_3) \in J_1 \times J_2 \times J_3$ ,  $\mathbf{w}(j_1) = \delta$ ,  $\mathbf{u}(j_2) = \delta$  and  $\mathbf{v}(j_3) = \delta$  for a constant  $\delta > 0$  and  $\mathcal{X}_{j_1, j_2, j_3} = 0$  for each  $(j_1, j_2, j_3)$  outside  $J_1 \times J_2 \times J_3$ . Concerning the noise mode, for  $(j_1, j_2, j_3) \in \bar{J}_1 \times \bar{J}_2 \times \bar{J}_3$ , we assume that the entries of  $\mathcal{Z}$  are i.i.d and have a standard normal distribution. This is the conventional noise model often considered in unsupervised learning method for tensor data [6,4].

### 3 Method

#### 3.1 Multi-slice clustering

Consider the triclustering problem (1). In the notation of Kolda and Bader [12], let

$$T_i = \mathcal{T}(i, :, :) = X_i + Z_i, \quad i \in [m_1] \quad (2)$$

be the horizontal (the first mode) matrix slice of the tensor  $\mathcal{T}$ , with  $X_i = \mathcal{X}(i, :, :)$  and  $Z_i = \mathcal{Z}(i, :, :)$ . Similarly, we can define the lateral (the second mode) and the frontal (the third mode) matrix slices. A way to learn the embedded triclustering in a real tensor data set is to find the similarity of the slices in each mode. This yields an index subset  $J_i$  for each mode. Now, the collection of  $J_i$  determines the tricluster.

**Definition 2 (Multi-slice clustering).** *The problem of multi-slice clustering of a 3-order tensor  $\mathcal{T}$  aims at determining and gathering the indices of the matrix slices that are similar in each dimension of the tensor.*

To illustrate the procedure, we will focus on the horizontal slices. The treatment of the other slices follows the same idea. We start by computing and performing a spectral analysis of

$$C_i = T_i^t T_i \quad (3)$$

for a fixed  $i \in [m_1]$ . For each  $i \in [m_1]$ ,  $C_i$  represents the symmetric covariance matrix of the  $i$ -th horizontal slice.

For  $i \in J_1$ , equation (1) shows that

$$C_i = (X_i + Z_i)^t (X_i + Z_i) = X_i^t X_i + X_i^t Z_i + Z_i^t X_i + Z_i^t Z_i \quad (4)$$

Taking into consideration (1) and (2), a tensor calculation shows that the matrix  $X_i^t X_i = \lambda_i \mathbf{v}_i \mathbf{v}_i^t$ , where  $\lambda_i = \gamma_i^2(\mathbf{w}(i))^2 > 0$  is the top eigenvalue of  $X_i^t X_i$  that corresponds to the top eigenvector  $\mathbf{v}_i$ . We re-express

$$C_i = \lambda_i \mathbf{v}_i \mathbf{v}_i^t + W_i \quad (5)$$

with  $W_i$  the remainder that can be inferred from expression (4). There is a perturbation bound that shows the norm difference between the top eigenvectors of  $C_i$  and  $\mathbf{v}_i$ , see section 4.

For  $i \notin J_1$ , the expression  $C_i$  (3) becomes the covariance of the noise slice:

$$C_i = Z_i^t Z_i \quad (6)$$

where each row of  $Z_i$  is real and independently drawn from  $\mathcal{N}_{m_3}(0, I)$ , the  $m_3$ -variate normal distribution with zero mean and covariance matrix  $I$ .

The covariance matrix  $C_i$  defines both the spread (variance) and the orientation (covariance) of our slice data. We are interested in the vector that represents the covariance matrix and its magnitude. The idea is to find the vector that points into the direction of the largest spread of the data  $(\lambda_i, \mathbf{v}_i)$ .

For each slice, the relation (3) holds for  $i = 1, \dots, m_1$ . Let  $\underline{\lambda}_i$  be the top eigenvalue and  $\tilde{\mathbf{v}}_i$  be the top eigenvector of  $C_i$ . We construct the matrix

$$V = [\tilde{\lambda}_1 \tilde{\mathbf{v}}_1 \cdots \tilde{\lambda}_{m_1} \tilde{\mathbf{v}}_{m_1}] \quad (7)$$

where we set  $\tilde{\lambda}_i$  to  $\underline{\lambda}_i/\lambda, \forall i \in [m_1]$ , and  $\lambda = \max(\underline{\lambda}_1, \dots, \underline{\lambda}_{m_1})$ . Let  $C$  be the matrix with each entry  $(c_{ij})_{i,j \in [m_1]}$  defined by

$$c_{ij} = |\langle \tilde{\lambda}_i \tilde{\mathbf{v}}_i, \tilde{\lambda}_j \tilde{\mathbf{v}}_j \rangle| = \tilde{\lambda}_i \tilde{\lambda}_j |\langle \tilde{\mathbf{v}}_i, \tilde{\mathbf{v}}_j \rangle| \leq 1 \quad (8)$$

$C$  is a symmetric matrix and its columns are not unit vectors. Note also that  $C$  is related to the covariance matrix  $V^t V$  in which we take the absolute values of the entries.

**Definition 3 ( $\epsilon$ -similarity).** We call the  $i^{\text{th}}$  and  $j^{\text{th}}$  slices  $\epsilon$ -similar, if for a small  $\epsilon > 0$  we have,

$$c_{ij} \geq 1 - \frac{\epsilon}{2} \quad (9)$$

Let  $\mathbf{d} = (d_1, \dots, d_{m_1})$  a real vector defined by the marginal sum in  $C$ :  $\forall i \in [m_1]$

$$d_i = \sum_{j \in [m_1]} c_{ij} \quad (10)$$

Using (9) and (10), the elements of  $J_1$  are some indices  $i \in [m_1]$  which define pairwise  $\epsilon$ -similar slices and therefore obeys

$$d_i \geq l(1 - \frac{\epsilon}{2}) \quad (11)$$

where  $l = |J_1|$ .

## 4 A perturbation bound on top eigenvectors

First, we recall a lemma withdrawn from [6]:

**Lemma 1.** Let  $Y = \mathbf{x}\mathbf{x}^t + \sigma W$ , where  $\mathbf{x} \in \mathbb{R}^n, \|\mathbf{x}\| = 1$  and  $W \in \mathbb{R}^{n \times n} = \sum_{j=1}^N (z_j z_j^T - \mathbb{E} z_j z_j^T)$  where  $z_j$  are i.i.d  $\mathcal{N}(0, I_{n \times n})$  gaussian random vectors. Let  $\tilde{\mathbf{x}} \in \mathbb{R}^n, \|\tilde{\mathbf{x}}\| = 1$  be the eigenvector corresponding to the largest eigenvalue of the matrix  $Y$ . Let the operator norm of the matrix  $W$  be such that

$$\|W\| \leq \eta_{n,N}, \quad (12)$$

with probability at least  $1 - \mathcal{O}(n^{-2})$ . Further, let

$$\sigma \leq \frac{c_0}{\eta_{n,N}}, \quad (13)$$

for some positive constant  $c_0 < 1/6$ . Letting  $M = \|\mathbf{x}\|_\infty$ , we have

$$\|\tilde{\mathbf{x}} - \mathbf{x}\|_\infty \leq \mathcal{O}\left(\sigma(\sqrt{N \log N} + M\eta_{n,N})\right) \quad (14)$$

with high probability as  $n \rightarrow \infty$ .

*Proof.* See lemma 6 in [6].

We will use the notation introduced for  $C_i = \lambda_i \mathbf{v}_i \mathbf{v}_i^t + W_i$  (5), given  $\lambda_i$  the top eigenvalue and  $\mathbf{v}_i$  the top eigenvector of  $X_i^t X_i$ . In the following  $n = m_3$ , to simplify our notation.

**Lemma 2.** Let  $\tilde{\mathbf{v}}_i$  be the top eigenvector  $C_i$ . There exists a bound on  $\|W_i\|$ , such that for  $\lambda_i = \mathcal{O}(n)$ , and  $\alpha = \|\mathbf{v}_i\|_\infty$ ,

$$\|\tilde{\mathbf{v}}_i - \mathbf{v}_i\|_\infty \leq \mathcal{O}\left(\frac{1}{\lambda_i} \alpha \log(n)\right) \quad (15)$$

holds with high probability as  $n \rightarrow \infty$ .

*Proof.* Let us focus on the noise term  $W_i = X_i^t Z_i + Z_i^t X_i + Z_i^t Z_i$ . Our goal is to select a suitable bound on it in such a way to fulfill the hypothesis of lemma 1.

$Z_i$  obeys a standard normal distribution, therefore  $\|Z_i\|$  is a sub-Gaussian random variable [20] and we have

$$\mathbb{P}(\|Z_i\| > t) \leq \exp(-ct^2) \quad (16)$$

Since

$$\begin{aligned} \|Z_i^t Z_i\| &= \sup_{\mathbf{y} \in S^{m_3-1}, \mathbf{x} \in S^{m_3-1}} \langle Z_i^t Z_i \mathbf{x}, \mathbf{y} \rangle = \sup_{\mathbf{y} \in S^{m_3-1}, \mathbf{x} \in S^{m_3-1}} \langle Z_i \mathbf{x}, Z_i \mathbf{y} \rangle \\ &= \sup_{\mathbf{x} \in S^{m_3-1}} \langle Z_i \mathbf{x}, Z_i \mathbf{x} \rangle = \|Z_i\|^2, \end{aligned} \quad (17)$$

we have  $\mathbb{P}(\|Z_i^t Z_i\| > t) \leq \exp(-ct)$ . Fix  $t = c' \log(n)$ , with  $c' > 2/c$ , to reach

$$\mathbb{P}(\|Z_i^t Z_i\| > c' \log(n)) \leq n^{-cc'}. \quad (18)$$

To have each entry of  $Z_i^t Z_i$  centered, we take  $Z_i^t Z_i - nI$  where  $I$  is the identity matrix of order  $n$ . Consequently, the mean of the noise is a scaled identity matrix, subtracting this term does not change the eigenvector structure.

Next, we bound the operator norm of  $X_i^t Z_i$  in probability. Each entries of  $X_i^t Z_i$  is a centered sub-gaussian random variable. We use again the same recipe. For a constant  $c > 0$  and  $t = c' \sqrt{\log(n)}$ ,  $c' > 2/c$ , we obtain

$$\mathbb{P}(\|X^t Z\| > c' \sqrt{\log(n)}) \leq n^{-cc'} \quad (19)$$

Combining (18) and (19), we get an upper bound of the noise term as

$$\|W_i\| \leq c'(\sqrt{\log(n)} + \log(n)) = \eta_{n,N} \quad (20)$$

that holds with probability  $1 - \mathcal{O}(n^{-cc'}) \geq 1 - \mathcal{O}(n^{-2})$ , as  $n$  goes to infinity.

We re-write  $C_i/\lambda_i = \mathbf{v}_i \mathbf{v}_i^t + W_i/\lambda_i$ , and set  $\sigma = 1/\lambda_i$ . We verify that

$$\sigma \leq \frac{c_0}{c'(\sqrt{\log(n)} + \log(n))} \quad (21)$$

which certainly occurs for large enough  $n$ . Then apply the  $l_\infty$ -perturbation bound of lemma 1 to deduce that for  $\hat{\mathbf{v}}_i$  the top  $C_i/\lambda_i$  that

$$\|\hat{\mathbf{v}}_i - \mathbf{v}_i\|_\infty \leq \mathcal{O}\left(\sigma(0 + M\eta_{n,N})\right) \leq \mathcal{O}\left(\frac{1}{\lambda_i} \alpha \log(n)\right) \quad (22)$$

after fixing  $N = 1$ ,  $\eta_{n,1} = c'(\sqrt{\log(n)} + \log(n))$ ,  $M = \alpha = \|\mathbf{v}_i\|_\infty$ . The same holds for  $\hat{\mathbf{v}}_i$  top eigenvector of  $C_i$ .  $\square$

## 5 Proofs of theorems

### 5.1 Fundamental lemma on TW distribution

For  $i \notin J_1$ , i.e. out of the cluster,  $C_i$  (3) becomes the covariance of the pure noise slice:

$$C_i = Z_i^t Z_i \quad (23)$$

where each row of  $Z_i$  is a real matrix independently drawn from  $\mathcal{N}_{m_3}(0, I)$ .  $C_i$  has a white Wishart distribution  $\mathcal{W}_{m_3}(m_2, I)$  [11]. It is also known that, at large  $m_2$  and large  $m_3$ , such that  $m_2/m_3 \rightarrow \gamma > 1$ , the largest eigenvalue distribution  $\lambda_i$  of  $C_i$  fulfills at the limit the following:

$$\frac{\lambda_i - \mu_{m_2 m_3, 1}}{\sigma_{m_2 m_3, 1}} \xrightarrow{\mathcal{D}} F_1 \quad (24)$$

where  $F_1$  is the Tracy-Widom (TW) cumulative distribution function (cdf), with parameters

$$\begin{aligned} \mu_{m_2 m_3, 1} &= (\sqrt{m_2 - 1} + \sqrt{m_3})^2 \\ \sigma_{m_2 m_3, 1} &= \sqrt{\mu_{m_2 m_3, 1}} \left( \frac{1}{\sqrt{m_2 - 1}} + \frac{1}{\sqrt{m_3}} \right)^{\frac{1}{3}} \end{aligned} \quad (25)$$

In [11], there could be a limit such that (24) still holds if  $m_2 < m_3$ , both  $m_2$  and  $m_3$  still going to infinity, and if the role of  $m_2$  and  $m_3$  are reversed in the expression of  $\mu_{m_2 m_3, 1}$  and  $\sigma_{m_2 m_3, 1}$ . It is also claimed that (24) is valid at the limit, with a satisfactory approximation whenever  $m_2, m_3 \geq 10$ . We will be above that range for these parameters in our next computations. We will drop the subscript  $(m_2 m_3, 1)$ , and simply write  $\mu = \mu_{m_2 m_3, 1}$  and  $\sigma = \sigma_{m_2 m_3, 1}$ .

The gamma distribution approximates the TW and is given by the following probability density function [10]

$$p(x) = \frac{(x - x_0)^{k-1}}{\theta^k \Gamma(k)} \exp \left[ -\frac{(x - x_0)}{\theta} \right] \quad (26)$$

where  $x_0 = -9.8209$  is the location (shift) parameter,  $k = 46.5651$  calls the shape,  $\theta = 0.1850$  the scale and  $\Gamma(k)$  the Gamma function. This mean of this random variable equals  $k\theta + x_0$ .

The following lemma is crucial in the proof of theorem 1.

**Lemma 3.** *Let  $Z_i$  be a  $M \times N$  matrix for  $i \in [n]$  where for each  $i$ , each row of  $Z_i$  is real and independently  $N$ -variate normal distribution with zero mean and covariance matrix  $I$ . Then the  $N \times N$  matrix  $Y_i = Z_i^t Z_i$  has a white Wishart distribution  $\mathcal{W}_N(M, I)$ . Denote  $\lambda_1, \dots, \lambda_n$  be the largest eigenvalue of  $Y_i$  for  $i \in [n]$ . For  $\mathbf{a} = (a_1, \dots, a_n)$  such that  $\forall i, a_i \geq 0$ ,*

– if  $\sum_i^n a_i \leq 1$ , for  $\lambda = \Omega(\mu)$ , we have

$$\frac{1}{\lambda} \sum_{i=1}^n a_i \lambda_i \leq \sqrt{\log(n)} \quad (27)$$

with probability at least  $1 - en^{-c_1}$  for a constant  $c_1 > 0$ .

– if  $1 < \sum_i^n a_i \leq n$ , for  $\lambda = \Omega(n\mu)$ , we have

$$\frac{1}{\lambda} \sum_{i=1}^n a_i \lambda_i \leq \sqrt{n} \quad (28)$$

with probability at least  $1 - en^{-c_2}$  for a constant  $c_2 > 0$ .

*Proof.* By definition of Wishart distribution with the gamma approximation of TW random variable, we know that  $\frac{\lambda_i - \mu}{\sigma} \xrightarrow{\mathcal{D}} F_1$ . The expected value of the TW for real random variable is equal to  $k\theta + x_0$ . For  $t > 0$  we have

$$\begin{aligned} \mathbb{P}\left(\left|\sum_i a_i \left(\frac{\lambda_i - \mu}{\sigma} - k\theta - x_0\right)\right| \geq t\right) &\geq \mathbb{P}\left(\sum_i a_i \left(\frac{\lambda_i - \mu}{\sigma} - k\theta - x_0\right) \geq t\right) \\ &\geq \mathbb{P}\left(\sum_i a_i \lambda_i \geq t\sigma + \left[\sigma(k\theta + x_0) + \mu\right] \sum_i a_i\right) \\ &\geq \mathbb{P}\left(\frac{1}{\lambda} \sum_i a_i \lambda_i \geq \frac{t\sigma}{\lambda} + \frac{\left[\sigma(k\theta + x_0) + \mu\right]}{\lambda} \sum_i a_i\right) \\ &\geq \mathbb{P}\left(\frac{1}{\lambda} \sum_i a_i \lambda_i \geq \frac{t\sigma}{\lambda} + \frac{(\sigma k\theta + \mu)}{\lambda} \sum_i a_i\right) \end{aligned} \quad (29)$$

For  $\sum_i a_i \leq 1$ , we have

$$\mathbb{P}\left(\left|\sum_i a_i \left(\frac{\lambda_i - \mu}{\sigma} - k\theta - x_0\right)\right| \geq t\right) \geq \mathbb{P}\left(\frac{1}{\lambda} \sum_i a_i \lambda_i \geq \frac{t\sigma}{\lambda} + \frac{(\sigma k\theta + \mu)}{\lambda}\right) \quad (30)$$

By hypothesis,  $\lambda = \Omega(\mu)$ , and take  $t = \sqrt{\mu \log(n)}$ , with

$$\frac{\sigma k\theta}{c\mu} = \frac{k\theta}{c\sqrt{\mu}} \left(\frac{1}{\sqrt{M-1}} + \frac{1}{\sqrt{N}}\right)^{\frac{1}{3}} \quad (31)$$

$$\frac{t\sigma}{c\mu} = \left(\frac{1}{\sqrt{M-1}} + \frac{1}{\sqrt{N}}\right)^{\frac{1}{3}} \frac{\sqrt{\log(n)}}{c} \quad (32)$$

For  $c > 2$ , we have  $\frac{t\sigma}{\lambda} + \frac{(\sigma k\theta + \mu)}{\lambda} \leq \sqrt{\log(n)}$ , then

$$\mathbb{P}\left(\frac{1}{\lambda} \sum_i a_i \lambda_i > \frac{t\sigma}{\lambda} + \frac{(\sigma k\theta + \mu)}{\lambda}\right) \geq \mathbb{P}\left(\frac{1}{\lambda} \sum_i a_i \lambda_i \geq \sqrt{\log(n)}\right) \quad (33)$$

Using proposition 5.10 [20] (Hoeffding-type inequality), with  $\sigma_m = \max_i \left\| \frac{\lambda_i - \mu}{\sigma} \right\|_{\psi_2}$  and for  $c > 0$  an absolute constant,

$$\mathbb{P}\left(\frac{1}{\lambda} \sum_i a_i \lambda_i \geq \sqrt{\log(n)}\right) \leq e \exp\left(\frac{-c\mu \log(n)}{\sigma_m \|a\|_1^2}\right) \leq e \exp\left(\frac{-c\mu \log(n)}{\sigma_m}\right) \quad (34)$$

We introduce  $c_1 = c \frac{\mu}{\sigma_m} > 0$ , and therefore

$$\frac{1}{\lambda} \sum_i a_i \lambda_i \leq \sqrt{\log(n)}$$

holds with probability at least  $1 - en^{-c_1}$ .

We now address the second statement (28). For  $1 < \sum_i a_i \leq n$ , we have

$$\mathbb{P}\left(\frac{1}{\lambda} \sum_i a_i \lambda_i > \frac{t\sigma}{\lambda} + \frac{(\sigma k\theta + \mu)}{\lambda} \sum_i a_i\right) \geq \mathbb{P}\left(\frac{1}{\lambda} \sum_i a_i \lambda_i > \frac{t\sigma}{\lambda} + \frac{(\sigma k\theta + \mu)}{\lambda} n\right) \quad (35)$$

By hypothesis,  $\lambda = \Omega(\mu n)$ , and take  $t = \mu n^{\frac{3}{2}}$ . For  $c > 2$ , we have  $\frac{(\sigma k\theta + \mu)}{\lambda} \leq \sqrt{n}$ , then

$$\mathbb{P}\left(\frac{1}{\lambda} \sum_i a_i \lambda_i > \frac{t\sigma}{\lambda} + \frac{(\sigma k\theta + \mu)}{\lambda} n\right) \geq \mathbb{P}\left(\frac{1}{\lambda} \sum_i a_i \lambda_i > \sqrt{n}\right). \quad (36)$$

We make use, once again, of proposition 5.10 in [20], with the same above  $\sigma_m$ , and for  $c > 0$  an absolute constant,

$$\mathbb{P}\left(\frac{1}{\lambda} \sum_i a_i \lambda_i \geq \sqrt{n}\right) \leq e \exp\left(\frac{-c\mu^2 n^3}{\sigma_m \|a\|_1^2}\right) \leq e \exp\left(\frac{-c\mu^2 n}{\sigma_m}\right) \quad (37)$$

Then, setting  $c_2 = c \frac{\mu^2}{\sigma_m} > 0$ , we obtain that

$$\frac{1}{\lambda} \sum_i a_i \lambda_i \leq \sqrt{n}$$

holds with probability at least  $1 - e \exp(-c_2 n)$ . □

We are in position to prove our main statement.

## 5.2 Proof of theorem 1

**Theorem 1.** *Let  $l = |J_1|$ , assume that  $\sqrt{\epsilon} \leq \frac{1}{m_1 - l}$ .  $\forall i, n \in J_1$ , for  $\lambda = \Omega(\mu)$ , there is a constant  $c_1 > 0$  such that*

$$|d_i - d_n| \leq l \frac{\epsilon}{2} + \sqrt{\log(m_1 - l)} \quad (38)$$

holds with probability at least  $1 - e(m_1 - l)^{-c_1}$ .

*Proof.* We start by the expression (10). Let  $i, n \in J_1$ ,

$$d_n - d_i = \sum_{j \in J_1} (c_{nj} - c_{ij}) + \sum_{j \in \bar{J}_1} (c_{nj} - c_{ij}) \quad (39)$$

for  $j \in J_1$ , we have  $1 > c_{nj}, c_{ij} > 1 - \frac{\epsilon}{2}$

$$1 - (1 - \frac{\epsilon}{2}) = \frac{\epsilon}{2} \geq c_{ij} - (1 - \frac{\epsilon}{2}) \geq c_{ij} - c_{nj} \quad (40)$$

Using the same approach, we have  $\frac{\epsilon}{2} \geq |c_{ij} - c_{nj}|, \forall i, n \in J_1$ . We evaluate

$$\left| \sum_{j \in J_1} (c_{nj} - c_{ij}) \right| \leq l \frac{\epsilon}{2} \quad (41)$$

Concerning the second term in (39), we write

$$\begin{aligned}
\left| \sum_{j \notin J_1} (c_{nj} - c_{ij}) \right| &= \left| \sum_{j \notin J_1} (\tilde{\lambda}_n |\langle \tilde{\mathbf{v}}_n, \tilde{\mathbf{v}}_j \rangle| - \tilde{\lambda}_i |\langle \tilde{\mathbf{v}}_i, \tilde{\mathbf{v}}_j \rangle|) \tilde{\lambda}_j \right| \\
&\leq \left| \sum_{j \notin J_1} (|\langle \tilde{\lambda}_n \tilde{\mathbf{v}}_n - \tilde{\lambda}_i \tilde{\mathbf{v}}_i, \tilde{\mathbf{v}}_j \rangle|) \tilde{\lambda}_j \right| \\
&\leq \sum_{j \notin J_1} \|\tilde{\lambda}_n \tilde{\mathbf{v}}_n - \tilde{\lambda}_i \tilde{\mathbf{v}}_i\| \|\tilde{\mathbf{v}}_j\| \tilde{\lambda}_j \\
&= \sum_{j \notin J_1} \|\tilde{\lambda}_n \tilde{\mathbf{v}}_n - \tilde{\lambda}_i \tilde{\mathbf{v}}_i\| \tilde{\lambda}_j
\end{aligned} \tag{42}$$

By definition of indices  $n$  and  $i$ , (54) and (9), the following bound is found

$$\|\tilde{\lambda}_n \tilde{\mathbf{v}}_n - \tilde{\lambda}_i \tilde{\mathbf{v}}_i\|^2 = \tilde{\lambda}_n^2 + \tilde{\lambda}_i^2 - 2\langle \tilde{\mathbf{v}}_n, \tilde{\mathbf{v}}_i \rangle \leq \epsilon \tag{43}$$

Thus, for  $\sqrt{\epsilon} \leq \frac{1}{m_1 - l}$ ,  $\sum_{j \notin J_1} \|\tilde{\lambda}_n \tilde{\mathbf{v}}_n - \tilde{\lambda}_i \tilde{\mathbf{v}}_i\| \leq 1$ , using lemma 3 we have

$$\left| \sum_{j \notin J_1} (c'_{nj} - c'_{ij}) \right| \leq \sqrt{\log(m_1 - l)} \tag{44}$$

with probability at least  $1 - e(m_1 - l)^{-c_1}$  for a constant  $c_1 > 0$ . □

### 5.3 Proof of theorem 2

**Theorem 2.** For  $i \in \bar{J}_1$ , if  $\lambda = \Omega(\mu m_1)$ ,

$$d_i \leq \frac{l}{m_1} + \sqrt{\log(m_1 - l)} \tag{45}$$

with probability at least  $1 - e(m_1 - l)^{-c_1}$  with  $c_1 > 0$ .

*Proof.* Starting by (10), we recast  $d_i$  in the form  $d_i = \left( \sum_{r \in J_1} + \sum_{r \in \bar{J}_1} \right) \tilde{\lambda}_r \tilde{\lambda}_i |\langle \tilde{\mathbf{v}}_r, \tilde{\mathbf{v}}_i \rangle|$ . Then, we bound

$$\sum_{r \in J_1} \tilde{\lambda}_r \tilde{\lambda}_i |\langle \tilde{\mathbf{v}}_r, \tilde{\mathbf{v}}_i \rangle| = \tilde{\lambda}_i \sum_{r \in J_1} \tilde{\lambda}_r |\langle \tilde{\mathbf{v}}_r, \tilde{\mathbf{v}}_i \rangle| \leq \tilde{\lambda}_i \sum_{r \in J_1} \tilde{\lambda}_r \|\tilde{\mathbf{v}}_r\| \|\tilde{\mathbf{v}}_i\| \leq l \tilde{\lambda}_i$$

The second step uses [10], that states that the support of the pdf of  $F_1$  is within  $[x_0, 2k\theta + x_0]$ . Therefore, we have

$$\frac{\lambda_i}{\lambda} \leq \frac{\sigma(2k\theta + x_0) + \mu}{\lambda}. \tag{46}$$

Since  $\lambda = \Omega(\mu m_1)$ , then  $\frac{\sigma(2k\theta + x_0) + \mu}{\lambda} \leq \frac{1}{m_1}$ . Hence,

$$\sum_{r \in J_1} \tilde{\lambda}_r \tilde{\lambda}_i |\langle \tilde{\mathbf{v}}_r, \tilde{\mathbf{v}}_i \rangle| \leq \frac{l}{m_1}, \quad \sum_{r \in \bar{J}_1} \tilde{\lambda}_r \tilde{\lambda}_i |\langle \tilde{\mathbf{v}}_r, \tilde{\mathbf{v}}_i \rangle| \leq \tilde{\lambda}_i \sum_{r \in \bar{J}_1} \tilde{\lambda}_r \tag{47}$$

The previous inequality (46) leads us to

$$\tilde{\lambda}_i \sum_{r \in \tilde{J}_1} \tilde{\lambda}_r \leq \frac{1}{m_1} \sum_{r \in \tilde{J}_1} \tilde{\lambda}_r \quad \text{and} \quad \frac{|\tilde{J}_1|}{m_1} \leq 1 \quad (48)$$

Using lemma 3 with  $\lambda = \Omega(\mu m_1)$ , we come to

$$\sum_{r \in \tilde{J}_1} \tilde{\lambda}_r \tilde{\lambda}_i |\langle \tilde{\mathbf{v}}_r, \tilde{\mathbf{v}}_i \rangle| \leq \sqrt{\log(m_1 - l)} \quad (49)$$

with probability at least  $1 - e(m_1 - l)^{-c_1}$  for a constant  $c_1 > 0$ .  $\square$

## 6 Sufficient conditions for rank one matrix similarity

We discuss in this appendix a sufficient condition that minimizes the norm distance between the slices  $C_i$ . We use the notation  $\tilde{\lambda}_i$  for the normalized top eigenvalue and  $\tilde{\mathbf{v}}_i$  the top eigenvector of the matrix slice  $C_i$ .

**Proposition 1.** *Let two slices be coined by  $i$  and  $j$ . For  $\tilde{\lambda}_i = \tilde{\lambda}_j$ , and  $\langle \tilde{\mathbf{v}}_i, \tilde{\mathbf{v}}_j \rangle = 1$ ,  $\|C_i - C_j\|$  is minimal.*

*Proof.* Let  $\mathbf{x} = \tilde{\lambda}_i \tilde{\mathbf{v}}_i - \tilde{\lambda}_j \tilde{\mathbf{v}}_j$ . For  $i, j \in [m_1]$ ,

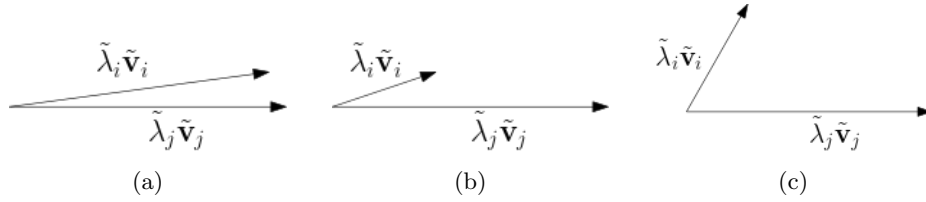


Fig. 2: Representation of the relation between the top eigenvectors and eigenvalues of the slice  $i$  and the slice  $j$ .

$$\begin{aligned} \|\tilde{\lambda}_i \tilde{\mathbf{v}}_i \tilde{\mathbf{v}}_i^t - \tilde{\lambda}_j \tilde{\mathbf{v}}_j \tilde{\mathbf{v}}_j^t\| &= \|\tilde{\lambda}_i \tilde{\mathbf{v}}_i \tilde{\mathbf{v}}_i^t - (\tilde{\lambda}_i \tilde{\mathbf{v}}_i + \mathbf{x})(\tilde{\lambda}_i \tilde{\mathbf{v}}_i + \mathbf{x})^t / \tilde{\lambda}_j\| \quad (50) \\ &= \|(\tilde{\lambda}_i - \frac{\tilde{\lambda}_i^2}{\tilde{\lambda}_j}) \tilde{\mathbf{v}}_i \tilde{\mathbf{v}}_i^t + \frac{\tilde{\lambda}_i}{\tilde{\lambda}_j} (\mathbf{x} \tilde{\mathbf{v}}_i^t + \tilde{\mathbf{v}}_i \mathbf{x}^t) + \frac{1}{\tilde{\lambda}_j} \mathbf{x} \mathbf{x}^t\| \\ &\leq \|(\tilde{\lambda}_i - \frac{\tilde{\lambda}_i^2}{\tilde{\lambda}_j}) \tilde{\mathbf{v}}_i \tilde{\mathbf{v}}_i^t\| + \|\frac{\tilde{\lambda}_i}{\tilde{\lambda}_j} (\mathbf{x} \tilde{\mathbf{v}}_i^t + \tilde{\mathbf{v}}_i \mathbf{x}^t)\| + \|\frac{1}{\tilde{\lambda}_j} \mathbf{x} \mathbf{x}^t\| \end{aligned}$$

For the first term, we have

$$\|(\tilde{\lambda}_i - \frac{\tilde{\lambda}_i^2}{\tilde{\lambda}_j}) \tilde{\mathbf{v}}_i \tilde{\mathbf{v}}_i^t\| = |\tilde{\lambda}_i - \frac{\tilde{\lambda}_i^2}{\tilde{\lambda}_j}| \|\tilde{\mathbf{v}}_i \tilde{\mathbf{v}}_i^t\| = |\tilde{\lambda}_i - \frac{\tilde{\lambda}_i^2}{\tilde{\lambda}_j}| \quad (51)$$

We deal with the second term:

$$\|\mathbf{x}\tilde{\mathbf{v}}_i^t\| = \sup_{\mathbf{u} \in S^{m_3-1}} \|\mathbf{x}\tilde{\mathbf{v}}_i^t\mathbf{u}\|_2 = \sup_{\mathbf{u} \in S^{m_3-1}} |\langle \tilde{\mathbf{v}}_i, \mathbf{u} \rangle| \|\mathbf{x}\|_2 = \|\mathbf{x}\|_2 \quad (52)$$

Likewise  $\|\tilde{\mathbf{v}}_i\mathbf{x}^t\| = \|\mathbf{x}\|_2$ . The third expression can be expressed as

$$\|\mathbf{x}\mathbf{x}^t\| = \sup_{\mathbf{u} \in S^{m_3-1}} \|\mathbf{x}\mathbf{x}^t\mathbf{u}\|_2 \quad (53)$$

The upper bound of (53) is reached at  $\mathbf{u} = \mathbf{x}/\|\mathbf{x}\|_2^2$ . Therefore,

$$\begin{aligned} \|\mathbf{x}\mathbf{x}^t\| &= \|\mathbf{x}\mathbf{x}^t \frac{\mathbf{x}}{\|\mathbf{x}\|_2^2}\|_2 = \|\mathbf{x}\|_2^2 \\ &= \tilde{\lambda}_i^2 + \tilde{\lambda}_j^2 - 2\tilde{\lambda}_i\tilde{\lambda}_j\langle \tilde{\mathbf{v}}_i, \tilde{\mathbf{v}}_j \rangle \end{aligned} \quad (54)$$

Thus to minimize (50), we inspect the following expressions:

$$\begin{cases} |\tilde{\lambda}_i - \frac{\tilde{\lambda}_i^2}{\tilde{\lambda}_j}| \\ \tilde{\lambda}_i^2 + \tilde{\lambda}_j^2 - 2\tilde{\lambda}_i\tilde{\lambda}_j\langle \tilde{\mathbf{v}}_i, \tilde{\mathbf{v}}_j \rangle. \end{cases} \quad (55)$$

To reach the minimum, we set  $|\tilde{\lambda}_i - \frac{\tilde{\lambda}_i^2}{\tilde{\lambda}_j}| = 0$  and that entails  $\tilde{\lambda}_i = \tilde{\lambda}_j$ . The second term is again set to 0 and we collect

$$\tilde{\lambda}_i^2 + \tilde{\lambda}_j^2 - 2\tilde{\lambda}_i\tilde{\lambda}_j\langle \tilde{\mathbf{v}}_i, \tilde{\mathbf{v}}_j \rangle = 0 \Rightarrow 2\tilde{\lambda}_i(1 - \langle \tilde{\mathbf{v}}_i, \tilde{\mathbf{v}}_j \rangle) = 0 \quad (56)$$

Therefore, the second condition for having a minimal norm between slices amounts to  $\langle \tilde{\mathbf{v}}_i, \tilde{\mathbf{v}}_j \rangle = 1$ .

□